

Energy partitioning over an irrigated vineyard in arid northwest China: Variation characteristics, influence degree, and path of influencing factors

Huiling Chen^a, Yongtai Zhu^b, Gaofeng Zhu^{b,*}, Yang Zhang^b, Liyang He^b, Cong Xu^b, Kun Zhang^c, Jing Wang^b, Ramamoorthy Ayyamperumal^b, Haochen Fan^b, Boyuan Wang^b

^a College of Geography and Environmental Science, Zhejiang Normal University, Jinhua 321004, China

^b College of Earth and Environmental Sciences, Lanzhou University, Lanzhou 730000, China

^c School of Geospatial Engineering and Science, Sun Yat-sen University, Zhuhai 519082, China

ARTICLE INFO

Keywords:

Energy partitioning
Vineyard
Arid advection
Influencing factors
Structural equation modeling

ABSTRACT

In this study, a two-year experiment in an irrigated vineyard was conducted to investigate the variations in energy fluxes (net radiation, R_n ; latent heat flux, LE; sensible heat flux, H ; and soil heat flux, G) and quantify the influence of arid advection and environmental factors (vapor pressure deficit (VPD), R_n , air temperature, wind speed, precipitation, and volumetric soil water content) on energy partitioning in arid Northwest China. For the diurnal variation, the peak values of the energy fluxes appeared at approximately 14:00, except for G (which appeared at approximately 16:00). LE was the main consumer of daytime ($R_n > 0$) energy during the growing season (average $LE/(R_n - G)$ was 87% and 89% in the two years), even during the shooting and leaf-fall stages. Arid advection, which affects energy partitioning mainly by increasing atmospheric evaporative demand and providing heat energy, contributed 6–60% and 1–56% of the average daytime LE during the two growing seasons, especially at the fruiting stage. Moreover, advection accounted for more than half of average daytime energy imbalances. We found that the arid advection induced by irrigation could be attenuated by selecting a reasonable irrigation time. According to the structural equation modeling (SEM) analysis, R_n had the strongest direct and positive regulation effect on LE at the half-hourly and daily scales, indicating that LE was limited by energy rather than water in the study area. The influence of R_n on LE gradually weakened with an increase in the time scale, whereas the effect of VPD increased, which may have been due to the smaller time-lag effect between VPD and LE. The diurnal variations in LE at approximately 08:00–19:30 and 19:30–08:00 were mainly controlled by the direct positive effects of R_n and VPD, respectively. The results obtained in this study will provide a better understanding of surface processes and help improve water resource management in arid agricultural areas.

1. Introduction

Energy exchange between terrestrial ecosystems and the atmosphere is a complex process, which drives hydrologic and biogeochemical cycles (Baldocchi et al., 2001). An agroecosystem, in particular, is a complex hydrological ecosystem involving energy, mass exchange, and the interaction of hydrological and ecological cycles caused by human activities in the various links to crop production (e.g., irrigation and cultivation) (Monteith et al., 2008; Ding et al., 2015). The study of farmland energy partitioning is crucial for understanding regional climate and water cycles (Mauder et al., 2020; Hossen et al., 2012), as well as the rational allocation and efficient utilization of water resources (Zhao et al., 2017; Zhang et al., 2016). The desert-oasis agroecosystem

plays a critical role in maintaining the ecological environment and stable agricultural productivity in desert areas (Zhang and Zhao, 2015). However, desert-oasis agroecosystems require long-term irrigation, and the heterogeneity of the underlying surface can complicate the energy exchange process (Wang et al., 2019). Thus, there is an urgent need to conduct an in-depth analysis of energy fluxes in a desert-oasis agroecosystem.

The eddy covariance (EC) technique has been recognized as the standard method for studying the water and energy exchange between the atmosphere and the surface (Liu et al., 2019; Baldocchi et al., 2004). To date, many studies of energy partitioning based on the EC technique have been conducted in different ecosystems, including grasslands (Liu et al., 2018; Krishnan et al., 2012; Eichelmann et al., 2016), forests (Yan

* Corresponding author.

E-mail address: zhugf@lzu.edu.cn (G. Zhu).

et al., 2017; Ma et al., 2018; Zhu et al., 2014), deserts (Yang and Zhou, 2011; Ma et al., 2014), wetlands (Liu et al., 2014; Zhao and Liu, 2018), and croplands (Liu et al., 2019; Gao et al., 2018; Zhang et al., 2016). In arid areas, the energy budget process of desert-oasis agroecosystems is usually more complicated due to the influence of atmospheric advection induced by surface heterogeneities and environmental factors (Morrison et al., 2022; Mauder et al., 2020; Cheng et al., 2014; Prueger et al., 1996, 2012; Wang et al., 2019). Arid advection can affect energy partitioning when the field becomes wetter and cooler than its surroundings, which is often the case for oases or irrigated areas (Díaz-Espejo et al., 2008; Tolk et al., 2006; Lei and Yang, 2010; Li and Yu, 2007). Previous studies have suggested that arid advection has a significant effect on energy fluxes and environmental factors in farmland areas and other regions (Lei and Yang, 2010; Morrison et al., 2022; Kool et al., 2018; Prueger et al., 1996; Kutikoff et al., 2019; Dare-Idowu et al., 2021; Li and Yu, 2007). However, few studies have investigated the variations of energy fluxes and the effects of environmental factors (e.g., vapor pressure deficit (VPD), net radiation (R_n), air temperature (Ta), wind speed (WS), precipitation (P), volumetric soil water content (VWC)) on energy partitioning in the desert-oasis irrigated vineyards of northwest China. In addition, the contribution of arid advection to energy exchange at the different crop phenological stages is still unclear and needs to be further investigated in vineyards under such conditions. Addressing these questions will help us to improve the scientific understanding of surface processes and water management in arid irrigated agricultural regions.

Furthermore, environmental variables are recognized as having a critical influence on energy partitioning (e.g., Zhu et al., 2014; Li et al., 2016; Li, 2015; Zhang et al., 2016). To date, the influence of environmental factors on energy partitioning has been investigated using two main methods: 1) multiple linear regression analysis, variance analysis, and correlation analysis (e.g., Zhao et al., 2017; Zhang et al., 2016; Alberto et al., 2011); and 2) through the use of certain diagnostic parameters (e.g., the decoupling coefficient Ω and Priestley-Taylor coefficient α ; Jiao et al., 2018; Liu et al., 2019; Xie et al., 2018; Baldocchi and Xu, 2007; Zhu et al., 2014). However, these methods have neither quantified the influence degree nor studied the influence path of environmental factors on energy partitioning. Fortunately, as a powerful technique for testing and evaluating multivariate causal relationships, structural equation modeling (SEM) can make up for the shortcomings of the above two methods: 1) the purpose of SEM is not to separate a single control factor from other factors, but to systematically study the overall influence of multiple factors; 2) it provides a way to divide the total effect into direct and indirect effects; and 3) it allows environmental factors to interact (Fan et al., 2016; Grace et al., 2012; Helman et al., 2017). Furthermore, some studies have shown that the main controlling periods for LE by R_n and VPD differ within a diel scale (0:00–24:00) (Baldocchi, 1994; Jia et al., 2018; Liu et al., 2021), but the specific period and influence path are still unclear. As a result, we decided to conduct research using SEM analysis to compensate for the deficiencies of the previous studies and to clarify the influence path and degree of influence of environmental factors on energy partitioning.

In the arid oasis areas of northwest China, grapes have been widely planted in recent years and have gradually become one of the main cash crops (Wang et al., 2019). In this study, given the aforementioned considerations, the energy components and environmental factors were measured using the EC technique in a vineyard in an arid region of northwest China in 2017 and 2018. Our scientific objectives were: 1) to investigate the dynamics of energy fluxes in the different crop phenological stages; 2) to quantify the contribution of arid advection to daytime energy partitioning in the different crop phenological stages; and 3) to clarify the influence path and degree of influence of environmental factors on energy partitioning at different time scales (half-hourly, daily, and diel scales).

2. Materials and methods

2.1. Study area

This study was conducted in a vineyard (*Vitis vinifera* cv. 'Thompson Seedless') ecosystem over the growing seasons in 2017 and 2018. The study area is located in the Nanhу Oasis of northwest China (94°06'19"E; 39°52'34"N; 1100–1300 m a.s.l.; Fig. 1a), which belongs to the temperate continental climate zone. The annual solar radiation in this area varies from 5903 to 6309 MJ m⁻², which provides sufficient sunlight for crop growth. The soil type is sandy loam. An area of 7.2 ha (160 m × 450 m) was selected in this study, which is surrounded primarily by Gobi Desert land (Fig. 1b). The wind direction in the study area is mainly from the northeast (Fig. 1b).

The mean height of the grape canopy is 2.5 m above the soil surface. Grapes were planted in rows with a spacing of 3 m (rows oriented from west to north and east to south). The distance between the grape trellises was 1 m (Fig. 1c). Weeds were removed periodically during the growing season. Pruning was conducted around day of the year (DOY) 200–220 in 2017 and 2018 to increase water use efficiency and improve yield. Flood irrigation was carried out once every 25 days, on average, which provided sufficient soil moisture to ensure normal growth of the grapes. Grapes were harvested once a year and their growing season is usually from late April or early May to late September or early October (Wang et al., 2019). Based on understanding the characteristics of grapes in each growth stage through field observations (i.e., comprehensive development characteristics, phenological characteristics, and leaf area changes), the growing season can be divided into five phenological stages, which are named the shooting (2017: DOY 121–147; 2018: DOY 117–150), fruiting (2017: DOY 148–171; 2018: DOY 151–168), filling (2017: DOY 172–222; 2018: DOY 169–219), maturity (2017: DOY 223–262; 2018: DOY 220–264), and leaf-fall (2017: DOY 263–283; 2018: DOY 265–282) stages.

In general, there were no apparent seasonal differences in environmental and physiological conditions between the two experimental periods (Fig. 2). The average values of Ta were 19.86 and 19.49 °C in 2017 and 2018, respectively (Figs. 2a and b). The mean VPD was 1.43 kPa in both years (Figs. 2a and b). Total P reached 25.4 mm (with one event greater than 10.0 mm) in 2017 and 16.51 mm (with no event greater than 10.0 mm) in 2018 (Figs. 2c and d). VWC was not sensitive to small rainfall events (less than 10.0 mm) and was mainly dependent on irrigation practices (Figs. 2c and d). The maximum VWC was reached after irrigation (about 0.28 and 0.23 m³ m⁻³ in 2017 and 2018, respectively) and gradually reduced until the next irrigation event. The daily mean WS varied from 0.19 to 1.78 m s⁻¹ and from 0.11 to 1.56 m s⁻¹ in 2017 and 2018, respectively (Figs. 2e and f). The leaf area index (LAI) increased gradually from the initial stage to the middle stage in both years and then decreased slowly. The maximum LAI reached 4.31 m² m⁻² on DOY 235 in 2017 (Fig. 2e) and 4.82 m² m⁻² on DOY 239 in 2018 (Fig. 2f). Moreover, photosynthetically active radiation (PAR) reached peak values (approximately 57 mol m⁻² day⁻¹) in early July, and the overall trend showed the characteristics of first increasing and then decreasing over both years (Figs. 2g and h).

2.2. Energy flux measurement, data processes, and energy balance closure

The latent heat flux (LE) and sensible heat flux (H) were measured using an EC system. This system can operate normally under complex and severe weather conditions and can provide accurate measurement data, and was installed in the middle of the experimental area at a height of 4 m above the ground (Fig. 1d). The system consisted of a three-dimensional sonic anemometer (R3–50, Gill Instruments, UK) and an open-path H₂O/CO₂ gas analyzer (LI-7500, LI-Cor Inc., Lincoln, NE, USA). Net radiation (R_n) was obtained from a radiation sensor (NR01, Hukse Flux, Delft, Netherlands), which was installed at a height of 3 m above the ground surface.

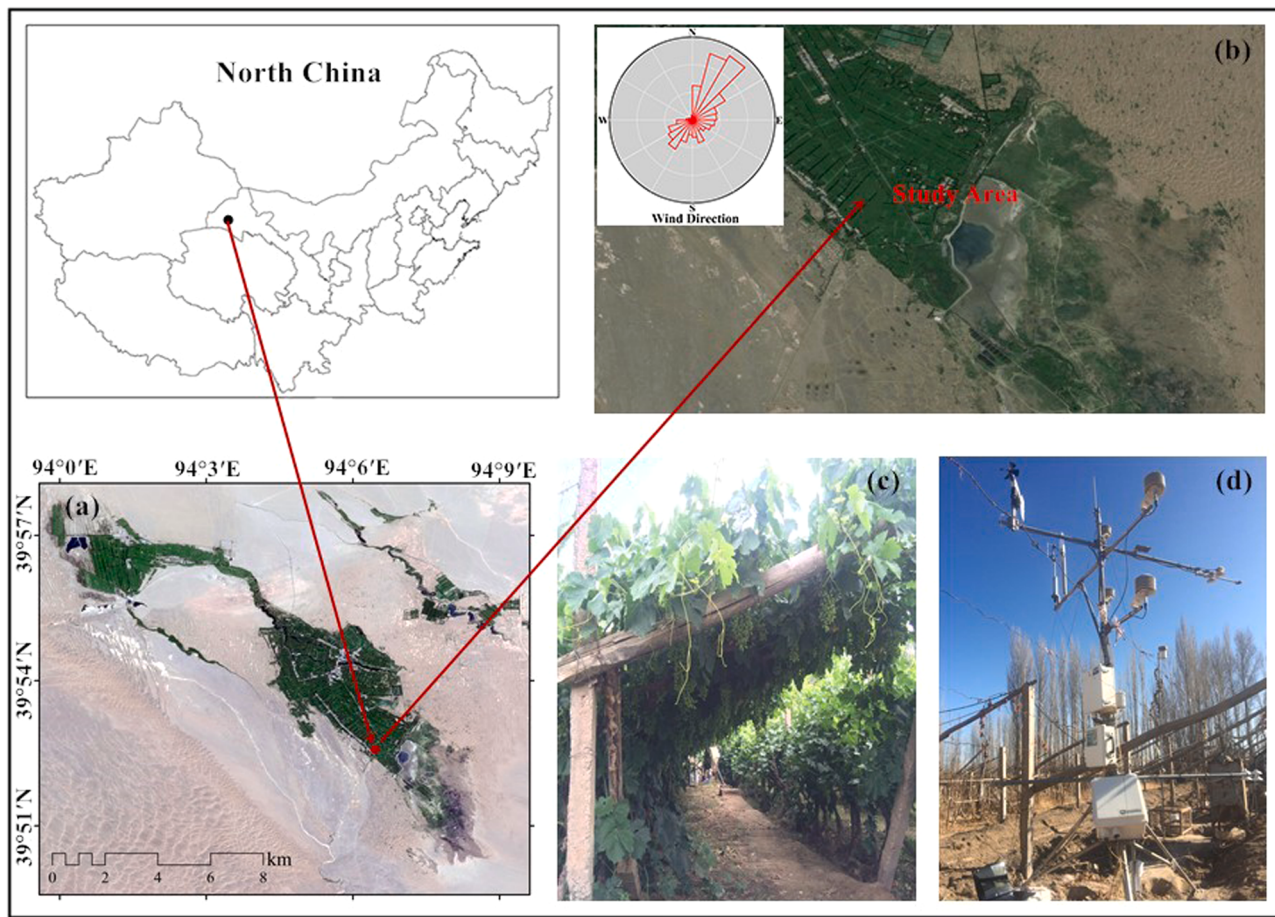


Fig. 1. Introduction to the study area and the observation instruments. (a) Location of the study area. (b) The surroundings and prevailing wind direction of the study area. (c) The vineyard and soil surface. (d) The eddy covariance (EC) and meteorological measurements used in this study.

In this study, the flux source area model (FSAM) footprint analysis model (Schmid, 1994) was used to analyze the source area of the flux footprint, and the results showed that the vineyards of interest primarily contributed to the measurements (Supplementary Text). All the above observations were recorded and stored using a data logger (CR1000, Campbell, USA), for which the collection time interval was 30 min. It is necessary to conduct correlation corrections when EC data are applied. Eddy Pro-software (version 6.0) was used to process and correct the original data collected by the EC system. A linear interpolation method was used when the data-loss period was less than 2 h per day. Measurements on rainy days were not used because the EC observations were uncertain. Furthermore, we used an artificial neural network to interpolate the rainy-day data to reveal the variation characteristics during the growing season more continuously because of the small number of rainfall days.

The soil heat flux (G) was calculated as follows (Oncley et al., 2007):

$$G = G_z + S_z \quad (1)$$

where G_z was measured using four heat flux plates (HFP01SC, Hukse Flux, Netherlands; two middle row positions, directly under the vine row) at a depth of 0.05 m below the ground surface. S_z is the soil heat stored above the heat flux plates, which can be estimated from:

$$S_z = c_{\text{soil}} z_p \frac{dT_{\text{soil}}}{dt} \quad (2)$$

$$c_{\text{soil}} = \rho_w \theta_v c_w + \rho_s c_s \quad (3)$$

where T_{soil} is the average temperature of the soil layer (calculated from

the soil temperature measurements at 0.01 m and 0.05 m depth), t is the time interval, c_{soil} is the heat capacity of moist soil, θ_v is the volumetric water content (estimated by measurement at 0.05 m, $\text{m}^3 \text{m}^{-3}$), ρ_w is the density of water, c_w is the water heat capacity, ρ_s is the bulk density of the soil, and c_s is the heat capacity of dry mineral soil.

The surface energy balance can be expressed as follows:

$$R_n = LE + H + G + Imb \quad (4)$$

Imbalance (Imb) is the total contribution of the neglected effects and uncertainties. Ideally, Imb should be zero; that is, the available energy ($R_n - G$) should be equal to the turbulent flux ($LE + H$). The energy balance closure was assessed using a linear regression between the available energy ($R_n - G$) and turbulent fluxes ($LE + H$) using half-hourly observations during the two experimental periods, excluding the values on rainy days and other exceptional cases. The results displayed a statistically significant fit and were robust for the half-hourly energy closure (slope = 0.90 and 0.91 with $R^2 = 0.82$ and 0.84 in 2017 and 2018, respectively; Fig. 3) and were comparable to the results obtained in grapevine ecosystems under similar circumstances in previous studies (Zhao et al., 2017; Ferreira et al., 2012). In general, energy balance residuals of 10–30% have been common in previous research (Foken, 2008; Allen et al., 2011), particularly in farmland ecosystems (Wilson et al., 2002). Therefore, the energy balance closure in this study was considered satisfactory.

2.3. Other variables

A small automatic weather station was installed in the study area to measure and record Ta, RH, WS, VWC, and PAR. Ta and RH were

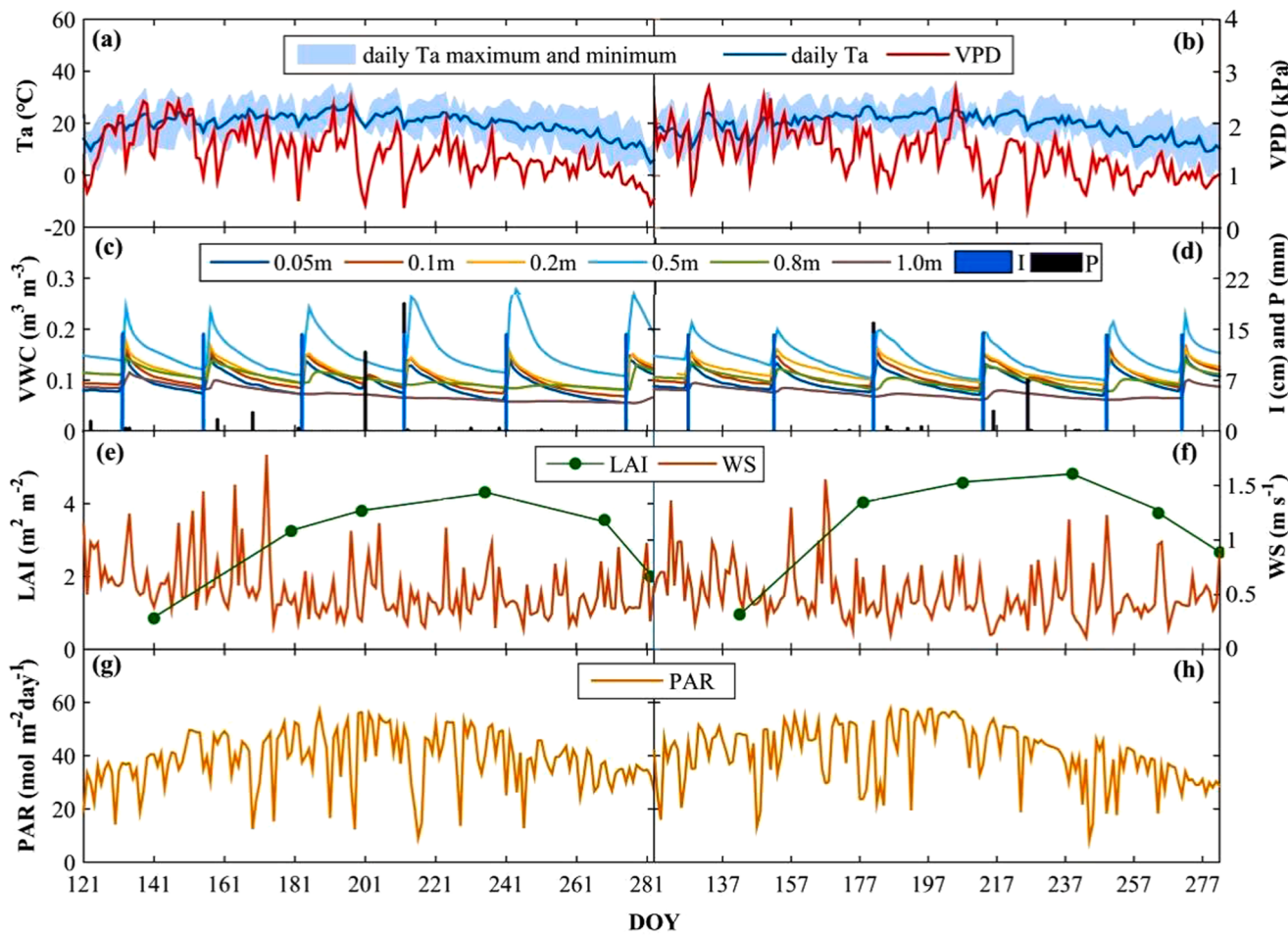


Fig. 2. Seasonal variations of ecological and environmental factors in 2017 (a, c, e, and g) and 2018 (b, d, f, and h): daily air temperature (Ta), vapor pressure deficit (VPD), volumetric water content (VWC) at different depths, precipitation (P) and irrigation amounts (I), wind speed (WS), leaf area index (LAI), and photosynthetically active radiation (PAR).

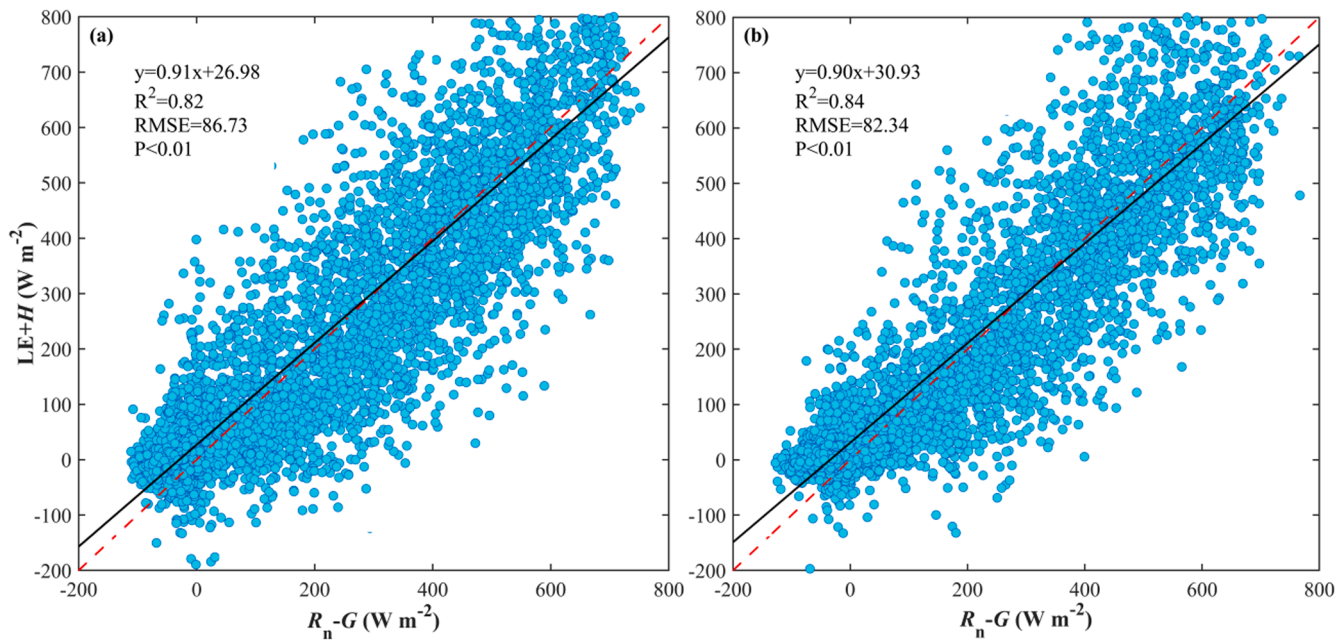


Fig. 3. Half-hourly energy balance closure analysis in the growing seasons of 2017 (a) and 2018 (b). The red dotted lines refer to $y = x$. The black lines indicate the regression equations. The X-coordinate is the available energy, and the Y-coordinate is the turbulent flux.

measured using temperature and humidity sensors (HMP60, Vaisala, Helsinki, Finland) at heights of 1.0, 1.5, 2.0, 2.5, and 3.0 m above the soil surface, and the mean value for the five heights was used in this study. PAR was measured at a height of 3 m using a quantum sensor (LI-190R; LI-Cor, USA). P was measured using a tipping bucket (TE525, Texas, USA). WS and wind direction were observed using a two-dimensional anemometer (5103, R. M. Young, USA) at a height of 0.5 m above the canopy. VWC and soil temperature were measured using soil moisture/temperature sensors (5TE, Decagon, USA) at depths of 0.05, 0.1, 0.2, 0.5, 0.8, and 1.0 m. Soil temperature at the top of the soil surface was measured using a soil temperature sensor (model 109-L, Campbell Scientific, Inc.) at a depth of 0.01 m. VPD was estimated from the RH and Ta. The LAI was measured monthly using an LAI-2200 canopy analyzer (Li-Cor).

2.4. Advection identification

We identified the occurrence of arid advection as either when the LE exceeded the available energy ($R_n - G$) or when H was negative during the daytime ($R_n > 0$). These indicators are similar to those used by Xu et al. (2017) and Kutikoff et al. (2019) and were originally discussed by Verma et al. (1978). This either/or definition was selected to account for measurement errors because the energy balance was not closed (Kutikoff et al., 2019). In this study, arid advection was identified at half-hour and daily scales (both during the daytime). It is worth noting that the arid advection identification at the daily scale was based on the average of the entire half-hour dataset during the daytime.

2.5. Parameter calculations

The contribution of arid advection (R_{ad}) to LE was calculated as follows (McNaughton et al., 1976; Priestley et al., 1972):

$$R_{ad} = \frac{LE - LE_{eq}}{LE} \quad (5)$$

where LE_{eq} is the required LE for equilibrium evapotranspiration of available energy contribution, i.e., without arid advection. LE_{eq} can be calculated by the following formula (McNaughton et al., 1983):

$$LE_{eq} = \frac{\Delta}{\Delta + \gamma} (R_n - G) \quad (6)$$

where Δ is the slope of the saturation vapor pressure-temperature curve, $\text{kPa } ^\circ\text{C}^{-1}$; γ is the hygrometer constant, $\text{kPa } ^\circ\text{C}^{-1}$.

The Priestley-Taylor coefficient (α) can be calculated by the following formula (Priestley and Taylor, 1972):

$$\alpha = \frac{LE}{LE_{eq}} = \frac{\Delta + \gamma}{\Delta} \frac{LE}{R_n - G} \quad (7)$$

The Bowen ratio (β) is equal to the ratio of H to LE, i.e.:

$$\beta = \frac{H}{LE} \quad (8)$$

2.6. Structural equation modeling (SEM)

SEM analysis is a powerful technique for testing and evaluating multivariate causal relationships and can test indirect and direct effects on pre-assumed causal relationships (Fan et al., 2016). Thus, we conducted an SEM analysis to clarify the influence path of environmental factors on LE at different time scales by reporting standardized path coefficients for the direct and indirect effects in the final path diagram (Fan et al., 2016; Grace et al., 2012). Generally, the establishment of SEM can be roughly divided into four steps: 1) constructing relationships between dependent and independent variables, 2) fitting the model, 3) testing the model, and 4) revising the model (Fan et al., 2016; Helman et al., 2017; Grace et al., 2012).

The environmental variables considered in this study were R_n , Ta, VPD, WS, VWC, and P . We first considered a full model that included all possible pathways (Fig. 4) and then sequentially eliminated non-significant pathways until we attained the final model. R_n provides the energy source for LE and also affects Ta and VPD; Ta has an effect on LE and VPD and is also affected by R_n and WS; VPD has an impact on LE and is also affected by R_n , WS, P , and Ta; and VWC has an impact on LE and is also affected by P (Chen et al., 2014; Zhang et al., 2016; Li et al., 2008; Liu et al., 2019; Law et al., 2002, 2020; Xie et al., 2018; Li, 2015; Wang et al., 2005). Irrigation was not considered in the SEM for two reasons: 1) We have already considered VWC in the SEM analysis; therefore, there is no need to add irrigation (VWC is mainly dependent on irrigation practices; Fig. 2). 2) The amount of irrigation data did not meet the sample size requirements. Based on the above, we obtained the assumptions behind the conceptualization of the SEM analysis (Fig. 4 and Eq. (9)).

$$\left\{ \begin{array}{l} LE = f(\text{half-hourly or daily } R_n, VPD, Ta, VWC, WS) \\ VPD = f(\text{half-hourly or daily } R_n, Ta, WS, P) \\ Ta = f(\text{half-hourly or daily } R_n, WS) \\ VWC = f(\text{half-hourly or daily } P) \end{array} \right. \quad (9)$$

Secondly, the unbiased maximum likelihood method was used for the parameter estimation, with 10,000 bootstrap resamples. Moreover, the SEM analysis was evaluated by relative and absolute fit indices, i.e., the normed fit index (NFI), comparative fit index (CFI), and root-mean-square error of approximation (RMSEA). The model was accepted when the indicators of $NFI > 0.95$, $CFI > 0.95$, $RMSEA < 0.1$, and the model did not contradict the relevant theory. Finally, the SEM was revised by modification indices (for which the thresholds were set to 4.0) and was theory-driven. In this study, the SEM analysis was conducted using software developed by SPSS, named Amos 26.0.

When the model was finally determined, the direct effects of the environmental factors on LE were assessed based on the standardized regression coefficients in Eq. (9). The indirect effects of the environmental factors on LE were calculated by multiplying the direct effects on the structural pathways (Qiu et al., 2019). By adding up the indirect and direct effects, the total effects of the environmental factors on LE were obtained. For example, R_n has a direct effect on LE, i.e., the path $R_n \rightarrow LE$. At the same time, there are indirect effects of R_n on LE, namely, paths

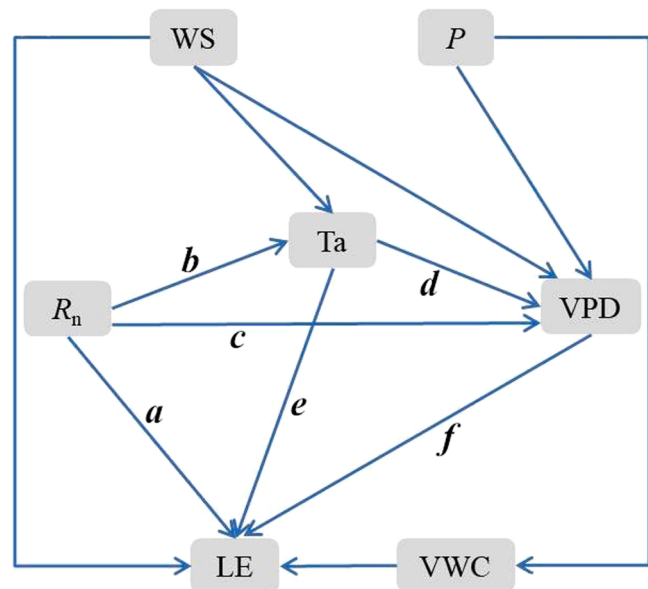


Fig. 4. Assumptions behind the conceptualization of the structural equation modeling (SEM) linking environmental variables and latent heat flux (LE).

$R_n \rightarrow Ta \rightarrow LE$, $R_n \rightarrow VPD \rightarrow LE$, and $R_n \rightarrow Ta \rightarrow VPD \rightarrow LE$ (Fig. 4). Therefore, the direct effect of R_n on LE is a ; and the indirect effect of R_n on LE is the sum of the two indirect paths (i.e., $b \times e + c \times f + b \times d \times f$).

SEM was selected to study the relationship between environmental factors and LE at three time scales: half-hourly, daily, and diel (0:00–24:00). In particular, we took the half-hourly interval and then took the data at the same time point in the entire study period as the sample for fitting the SEM when we analyzed the influence of environmental factors on LE at the diel scale.

3. Results

3.1. Energy partitioning in the different phenological stages

Fig. 5 illustrates the diurnal variations in the energy components on clear days during the growing season. Each energy component exhibits an inverted U-shaped characteristic. The maximum values of R_n occurred between 14:00 and 14:30 during the different phenological stages. LE showed a multi-peak characteristic in the first three growth stages and remained greater than zero at night. The maximum LE values occurred in the afternoon (between 13:00 and 14:00). Because more energy reaches the ground during the shooting stage than during the other stages, the diurnal variation in G was more evident in the shooting stage. Furthermore, G lagged behind R_n by an average of approximately 2 h (Zhang et al., 2007).

The seasonal variations of the average daytime $LE/(R_n-G)$, $H/(R_n-G)$, and Bowen ratio (β) are shown in Fig. 6 and Table 1. LE data were missing because of power and instrument failures from DOY 117 to 139 in 2018. Between the two experimental years, there were no significant differences in seasonal variations in average daytime energy partitioning. In general, $LE/(R_n-G)$ was nearly 1 over the entire growing season, with a minimum value of 0.70, occurring during the leaf-fall

stage in 2017, and a maximum value of 1.14, which occurred during the fruiting stage in 2018, indicating that LE was the main consumer of available energy during the growing season. The average values of $LE/(R_n-G)$ were 0.87 and 0.89 over the entire growing season (Figs. 6a and c; Table 1). $H/(R_n-G)$ showed an opposite variation to $LE/(R_n-G)$ and decreased rapidly from 0.51 during the shooting stage to nearly 0 during the fruiting, filling, and maturity stages in both years. Then, it increased to 0.26 and 0.25 during the leaf-fall stages in 2017 and 2018, respectively, due to the evaporative cooling effects. Consequently, the seasonal variation of β decreased from 0.88 to 0.70 during the shooting stage to nearly 0 during the fruiting, filling, and maturity stages, and then increased to 0.43 and 0.34 during the leaf-fall stage in 2017 and 2018, respectively (Fig. 6b; Table 1). G was small and changed slightly over the two years, with the mean value decreasing from 49.00 to 29.71 $W\ m^{-2}$ during the shooting stage to 15.72 and 8.25 $W\ m^{-2}$ in the leaf-fall stage (Supplementary Fig. 1 and Table 1). Because most solar radiation is absorbed by the canopy rather than the ground as the grapes grow, G decreased constantly during each growing season (Zhou et al., 2012).

3.2. Effect of arid advection on energy partitioning

The number of days with an average daytime $LE/(R_n-G)>1$ or $H/(R_n-G)<0$ was 49 and 54 in 2017 and 2018, respectively (Figs. 6a and c), indicating that the effect of arid advection on energy partitioning was notable (Kutikoff et al., 2019; Lee et al., 2004; Li and Yu, 2007). We calculated the contribution rate (R_{ad}) of arid advection to the LE to quantitatively analyze the intensity of arid advection and its influence on energy partitioning (Fig. 7). The average daytime R_{ad} ranged from 6% to 60% and 1% to 56%, with average values of 29% and 25%, over the entire growing season in 2017 and 2018, respectively (Fig. 7; Table 1), indicating that the effects of arid advection on the LE should not be ignored. Furthermore, arid advection accounted for more than

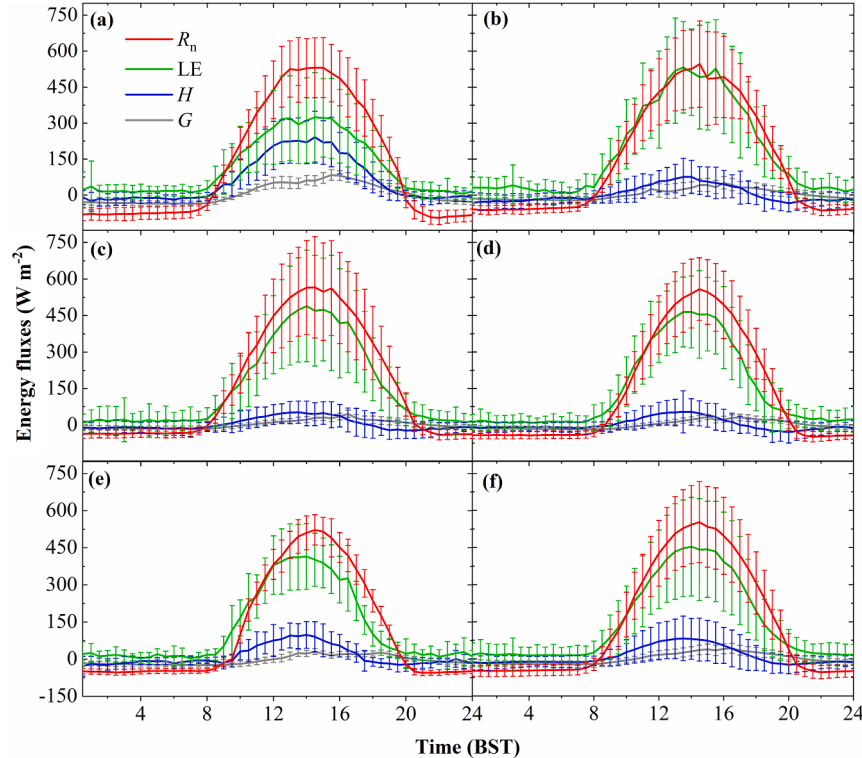


Fig. 5. Average diurnal variations in net radiation flux (R_n), latent heat flux (LE), sensible heat flux (H), and soil heat flux (G) on clear days for the different phenological stages: (a) the shooting stage; (b) the fruiting stage; (c) the filling stage; (d) the maturity stage; (e) the leaf-fall stage; and (f) the entire growing season at the study area. The error bars represent the standard deviation. Beijing Standard Time (BST) is used here.

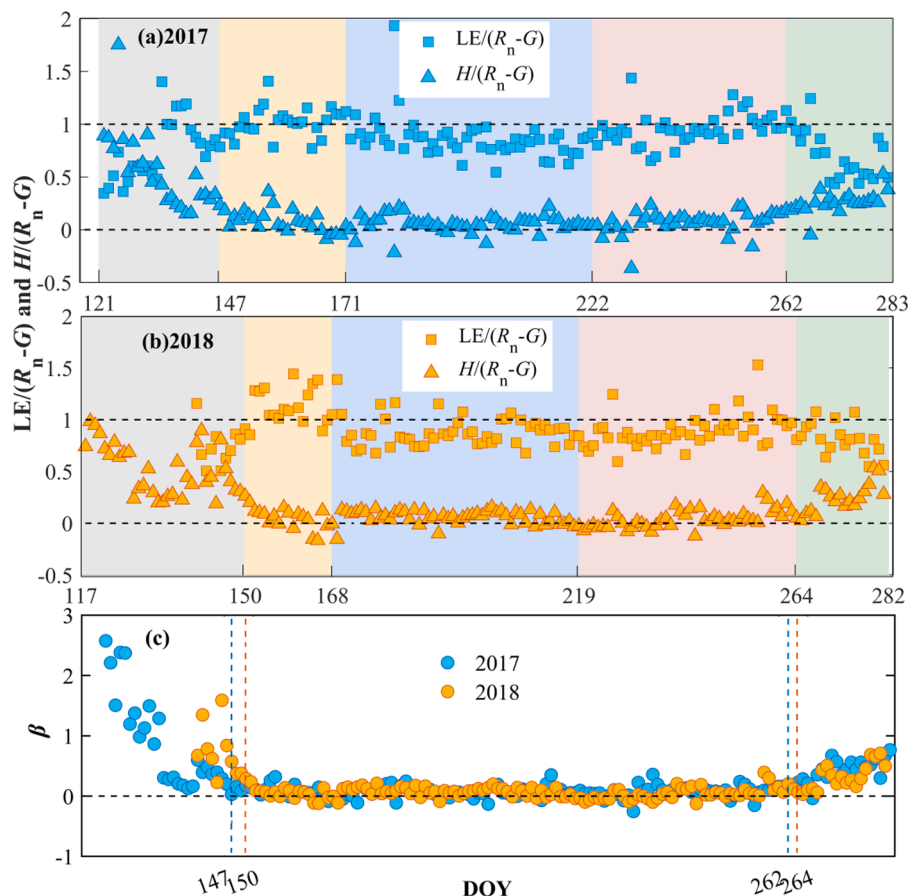


Fig. 6. Seasonal variations of daytime latent heat flux (LE) and sensible heat flux (H) as a percentage of available energy (R_n-G) and the Bowen ratio (β) in 2017 and 2018. The different color backgrounds in the figure indicate the different phenological stages, as listed in Table 1.

Table 1

Energy partitioning in the daytime at the different phenological stages and the entire growing seasons.

Year	Growth stage	Energy component(W m^{-2})				Energy ratio(%)			R_{ad} (%)
		R_n	LE	H	G	LE/ (R_n-G)	$H/(R_n-G)$	β	
2017	Shoot	341.37	232.36	132.02	49.00	0.77	0.51	0.88	35
	Fruiting	352.13	336.15	26.31	21.09	1.03	0.08	0.08	29
	Filling	370.86	300.92	19.21	17.26	0.86	0.05	0.07	23
	Maturity	330.63	296.06	25.75	16.22	0.96	0.07	0.08	31
	Leaf-fall	288.38	189.90	70.6	15.72	0.70	0.26	0.43	33
	Entire	342.72	279.25	47.17	22.63	0.87	0.16	0.25	29
2018	Shoot	277.61	218.88	123.57	29.71	0.75	0.51	0.70	\
	Fruiting	345.84	365.07	18.56	17.58	1.14	0.04	0.04	34
	Filling	357.76	304.26	21.30	12.17	0.88	0.07	0.07	22
	Maturity	349.29	296.01	12.46	9.57	0.89	0.04	0.05	23
	Leaf-fall	305.67	241.08	74.80	8.25	0.81	0.25	0.34	31
	Entire	332.11	294.80	45.35	15.22	0.89	0.17	0.14	25

half of the average daytime energy imbalance during the two years (Fig. 8).

We also investigated the differences in the advection intensity caused by irrigation at different times. Because of the high probability of arid advection in the early morning and late afternoon (Li and Yu, 2007), we selected the midday period (between 10:00 and 16:00) of three consecutive clear days (R_n in Fig. 9) in 2017 and four days in 2018 to study the differences in advection intensity caused by irrigation at different times (Fig. 9). After irrigation, more frequent and intense arid advection occurred during the subsequent midday period, indicating that irrigation was a key driving force for advection in arid areas (Fig. 9). As can be seen in Fig. 9, the average values of R_{ad} were 34% on DOY 157 (irrigation took place at night on DOY 156) in 2017 and 44% on DOY

152 (irrigation took place in the morning on DOY 152) in 2018. The duration of advection on DOY 157 (8 h) was also smaller than that on DOY 152 (11 h). Thus, irrigation should be conducted in the evening rather than in the morning because advection can lead to an ineffective loss of irrigation water. Compared to irrigation in the morning, irrigation in the evening enabled sufficient time for water to penetrate deeper, such that the surface water of the soil is significantly lower at noon the following day (Supplementary Fig. 2), thus reducing the heterogeneity of the vineyard and the surrounding environment.

3.3. Effect of environmental factors on latent heat flux

SEM analysis was used to explore the direct and indirect impacts of

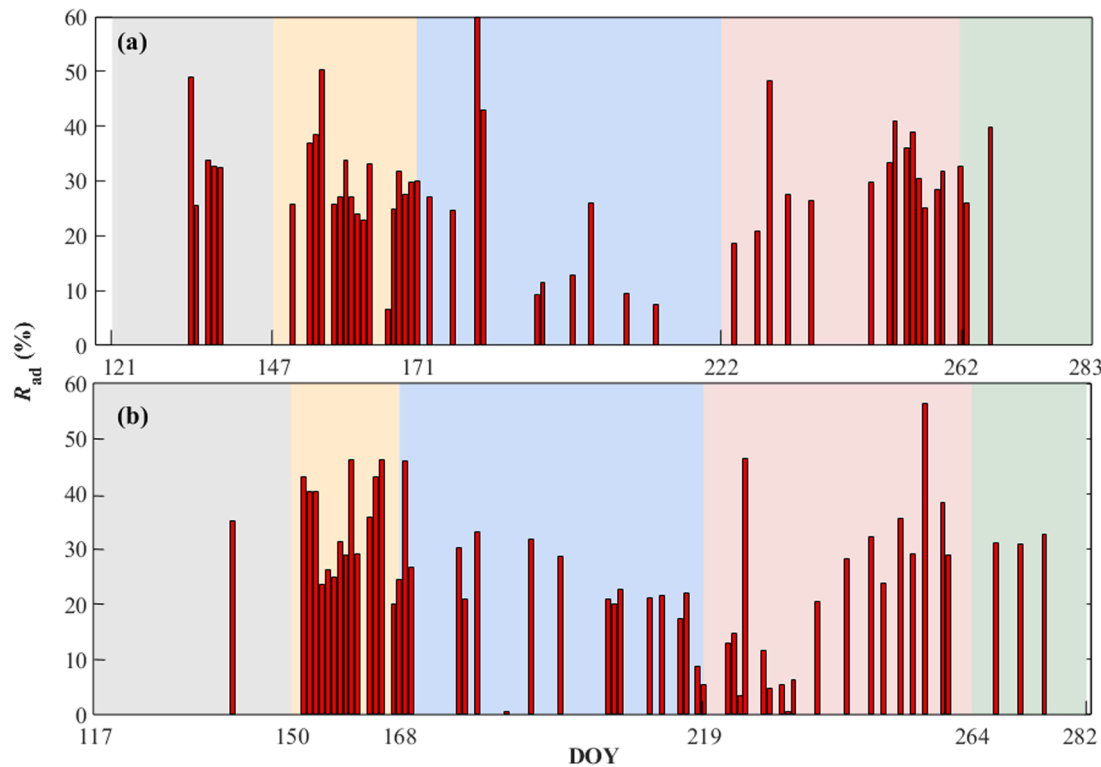


Fig. 7. Seasonal variations in the average daytime R_{ad} over the growing seasons in 2017 (a) and 2018 (b).

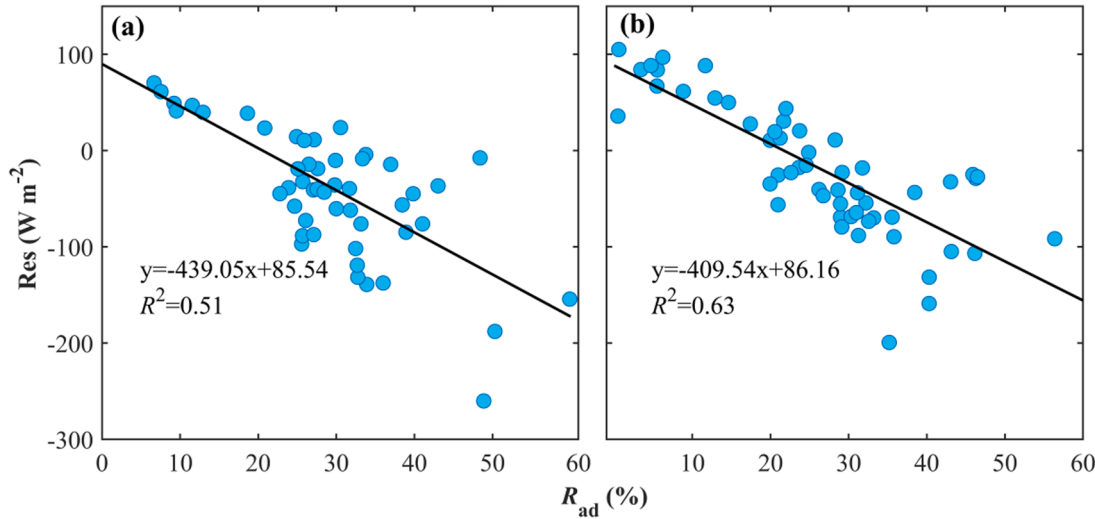


Fig. 8. Regression between the daily (average in the daytime) residual energy ($Res = R_n - LE - H - G$) and R_{ad} over the entire growing season in 2017 (a) and 2018 (b). The solid black lines represent the regression lines.

environmental factors on the LE at different time scales (Figs. 10–12). At the half-hourly scale, the SEM results showed that R_n , VPD, Ta, P, and WS explained 75% and 79% of the variation in LE in 2017 and 2018, respectively (Figs. 10a and b). The total effects of R_n , VPD, and WS on the LE were positive, whereas the total effects of P and Ta on the LE were negative. R_n had the largest direct and positive effect on LE (0.87 in 2017 and 0.84 in 2018), followed by VPD (0.09 in 2017 and 0.11 in 2018). VPD had only a weak positive impact on LE. Other factors (Ta, WS, and P) had little effect on LE at the half-hourly scale. Among these factors, WS is important due to the heterogeneity of the surrounding environment. At the half-hourly scale, WS had a significant positive effect on VPD (0.23 in 2017 and 0.24 in 2018) and Ta (0.19 in 2017 and 0.14 in

2018), indicating that the wind brings hot and dry air. Generally, R_n was the main driver of LE through direct and positive effects at the half-hourly scale during the growing season.

At the daily scale, the SEM analysis showed that environmental factors explained 75% and 74% of the variation in daily LE in 2017 and 2018, respectively (Figs. 11a and b). It is worth noting that the total effect of Ta was positive at this scale due to the enhanced indirect effect of Ta on daily LE through VPD (0.15 in 2017 and 0.17 in 2018). R_n and VPD showed significant direct and positive effects on LE, whereas the direct effect of Ta was not significant. The largest significant direct effect was from R_n (0.61 in 2017 and 0.63 in 2018), followed by VPD (0.35 in 2017 and 0.34 in 2018). However, compared to the half-hourly scale,

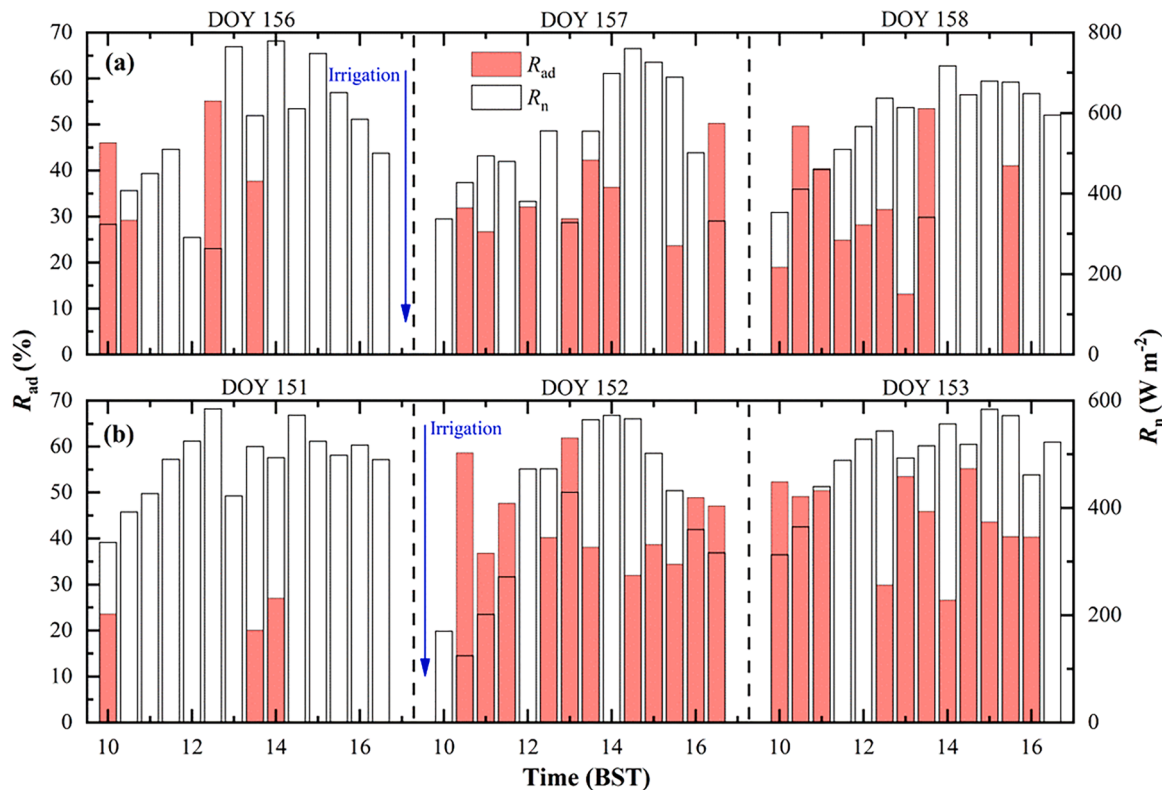


Fig. 9. Variations of the half-hourly R_{ad} at midday (10:00–16:00) before and after irrigation in 2017 (a) and 2018 (b). The irrigation event took place in the afternoon (18:00) on DOY 156 in 2017 and in the morning (08:00) on DOY 152 in 2018, with the water amount being 14.5 cm each time.

the effect of R_n on LE decreased (both direct and total effects), and the effect of VPD on LE increased (both direct and total effects) at the daily scale. In addition, the effect of WS on LE was greater than that at the half-hourly scale (total effect of 0.18 and 0.19 in 2017 and 2018, respectively). These results indicated that R_n and VPD mainly regulated daily LE through direct effects and Ta through indirect effects.

Fig. 12 depicts the dominant period and the main influence path of R_n and VPD on LE in a diel cycle (0:00–24:00). It is clear that R_n and VPD had different main controlling periods for the LE. From 19:30 to 08:00 (white area in Fig. 12), D_{VPD-LE} (D_{i-LE} represents the direct effect of factor i on LE) was larger than T_{Rn-LE} (T_{i-LE} represents the total effect of factor i on LE), indicating that the variation in LE during this period was mainly directly controlled by VPD. Moreover, from 08:00 to 19:30 (blue area in Fig. 12), T_{Rn-LE} was larger than D_{VPD-LE} , implying that R_n was the main contributor to the LE. During the same period, D_{Rn-LE} was greater than I_{Rn-LE} (I_{i-LE} denotes the indirect effect of i on LE) (Supplementary Fig. 3), implying that the variation of LE in this period was mainly directly controlled by R_n .

4. Discussion

4.1. Energy balance closure

The lack of energy balance closure in micrometeorological studies is still a hot and unsolved problem (Mauder et al., 2020). In general, energy balance residuals of 10–30% were common in previous research (Foken, 2008; Allen et al., 2011; Zhang et al., 2016), particularly in farmland ecosystems (Wilson et al., 2002). In our study, the slopes were 0.91 and 0.90, and the intercept values were 26.98 and 30.93 W m^{-2} in the two years (Fig. 3). Therefore, the energy balance closure in this study area was satisfactory compared to previous findings, implying that the EC system provides a reliable basis for this research. However, it must be stressed that there is still a residual energy balance of approximately 10%.

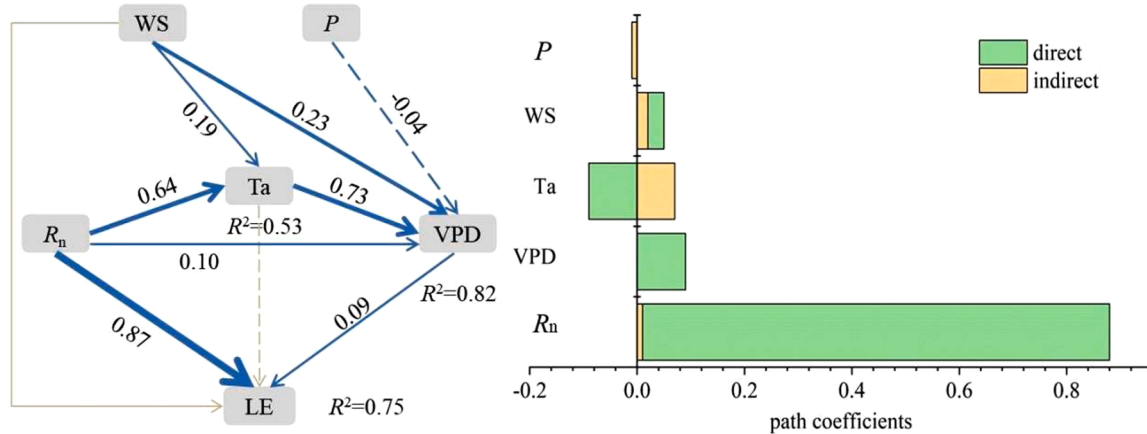
Scientists have used advection as a proxy for spatial heterogeneity and have found that arid advection has effects on energy balance closure, especially at the hectometer and kilometer scales (Morrison et al., 2022; Mauder et al., 2020; De Roo and Mauder, 2018; Prueger et al., 2012; Cuxart et al., 2016; Kool et al., 2018). In this study, the surrounding environment, meteorological conditions, and agricultural practices such as irrigation caused intense arid advection (Fig. 7), which accounted for more than half of the average daytime energy imbalance over the two years (Fig. 8). Dare-Idowu et al. (2021) reported similar results. Furthermore, as shown in Fig. 8, with the increase of advection intensity, the energy balance residual first approached zero and then became increasingly negative. This indicates that arid advection brings heat energy to the surrounding environment, which is also reflected in the SEM results, indicating that WS had a significant direct and positive effect on Ta and LE (Figs. 10 and 11).

Furthermore, researchers are also considering how to use the residual Imb (Eq. (4)) to correct the measured turbulent heat fluxes, i.e., how to divide the residual between LE and/or H . There are three opinions on this topic: 1) The residual is partitioned between H and LE (e.g., Foken, 2008; Mauder et al., 2020). There are theoretical arguments in favor of forcing energy balance closure, i.e., attributing the energy imbalance to H and LE so that the Bowen ratio remains unchanged (Foken, 2008). 2) The entire residual is attributed to the LE (e.g., Wohlfahrt et al., 2010). 3) The entire residual is attributed to H (e.g., Ingwersen et al., 2011). Among the above three viewpoints, we believe that the first is suitable for our study area (i.e., a desert-oasis agroecosystem) because strong advection (including horizontal and vertical advection) usually causes H and LE to simultaneously exert effects on the energy balance of the irrigated farmland at the same time (Cuxart et al., 2016; Kool et al., 2018).

4.2. Energy partitioning during the growing season

Understanding the variations in energy fluxes is critical for

(a) CFI=0.99, NFI=0.98, RMSEA=0.01, Sample size=6864, P=0.17



(b) CFI=0.99, NFI=0.99, RMSEA=0.01, Sample size=6864, P=0.16

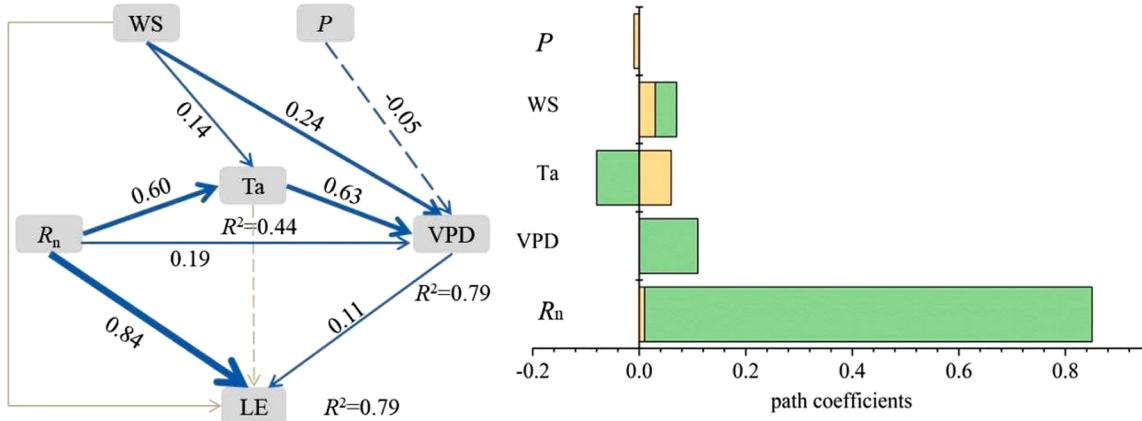


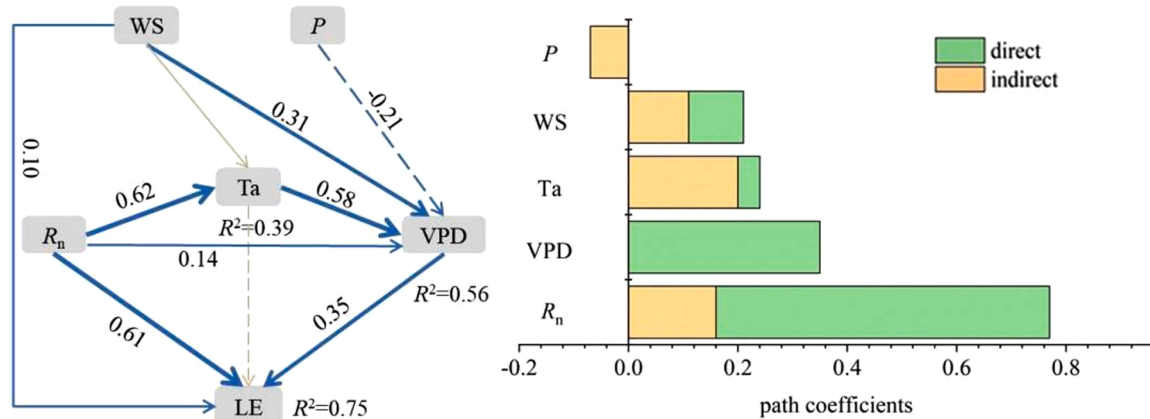
Fig. 10. Structural equation models for latent heat flux (LE) at the half-hourly scale over the entire growing season in 2017 (a) and 2018 (b). The blue lines represent significant paths ($P < 0.05$); the gray lines indicate non-significant paths ($P > 0.05$); the solid (dotted) lines indicate positive (negative) paths. The numbers are the standard path coefficients, and the width of the line is proportional to the path coefficient. The bar diagrams show the standardized path coefficients of the environmental variables on LE. Abbreviations: R_n : net radiation; Ta: air temperature; VPD: vapor pressure deficit; WS: wind speed; P: precipitation; NFI: normed fit index; CFI: comparative fit index; RMSEA: root-mean-square error approximation.

understanding the exchange of water and energy between vineyards and the atmosphere. In this study, the energy balance components showed a typical diurnal pattern (i.e., an inverted U-shape; Fig. 5), which is consistent with that of most ecosystems (e.g., Zhu et al., 2014; Zhang et al., 2007). The SEM results showed that R_n mainly controls the diurnal variation in LE during the day (Fig. 11); therefore, the diurnal variations in R_n and LE were synchronous (Fig. 5). LE showed a multi-peak characteristic in the first three phenological stages (Figs. 5a-c), which may have been due to intense solar radiation causing grape leaves to close their stomata autonomously to prevent excessive water loss. At night, the LE was greater than zero, which may have been due to high VPD (Balocchi, 1994; Fig. 12) or weak advection (Hanks et al., 1971).

The seasonal variations in energy partitioning in both years were similar: LE/($R_n - G$) showed an upward trend and then a downward trend each year, which was opposite to $H/(R_n - G)$, and G showed a downward trend each year (Table 1). The LAI played a key role in these seasonal variations. LAI determines the transpiration of grape plants, thus affecting the partitioning of R_n into LE and H . Meanwhile, the change in LAI determines the proportion of R_n reaching the ground, which affects the change in G . The average LE/($R_n - G$) was 0.87 and 0.89 in the growing seasons of the two years. Therefore, LE was the main consumer of available daytime energy, similar to the results of previous studies on wheat fields in the North China Plain (Lei et al., 2010), irrigated maize

fields in the United States (Suyker and Verma, 2008), and maize fields in arid northwest China (Ding et al., 2014; Zhang et al., 2016). We found that even during the shooting stage, LE was the main consumer of available energy, mainly because soil evaporation played a major role during this period (Wang et al., 2019). This apparent soil evaporation was mainly due to adequate irrigation and high R_n (Figs. 2 and 11). However, some scholars have studied the energy partitioning of grape farmlands in different geographical environments and found that H always occupies the majority of the available energy (e.g., Zhang et al., 2007; Yu et al., 2020). Moreover, the average $H/(R_n - G)$ was 0.16 and 0.17 during the two growing seasons, which is lower than in other studies (e.g., Zhang et al., 2016; Zhu et al., 2014, 2007; Yu et al., 2020). The partitioning of R_n into LE and H for a vineyard area is determined by the irrigation practices and meteorological conditions (Spano et al., 2004). In the study area, adequate irrigation allowed grape growth without water limitation, and the atmospheric evaporative demand was high (Fig. 2). The different energy consumption patterns of grape plants in different geographical locations can be attributed to the differences in their management practices (e.g., irrigation scheduling and planting density) and environmental conditions (e.g., arid advection and environmental factors) (Balocchi et al., 2004; Kool et al., 2016). Therefore, it is important to understand how influencing factors affect energy partitioning during the seasons.

(a) CFI=0.99, NFI=0.98, RMSEA=0.06, Sample size=143, P=0.13



(b) CFI=0.97, NFI=0.96, RMSEA=0.07, Sample size=143, P=0.14

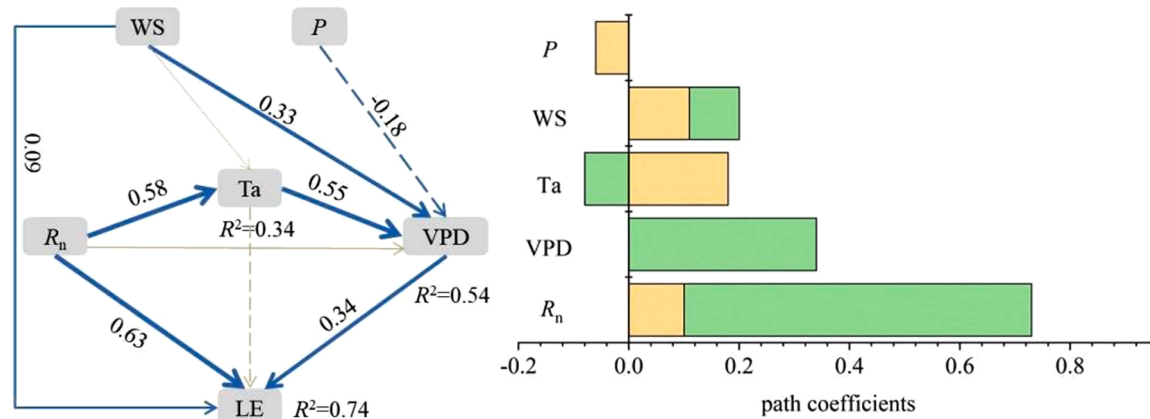


Fig. 11. Structural equation models for latent heat flux (LE) at the daily scale during the entire growing season in 2017 (a) and 2018 (b). Other details are as shown in Fig. 10.

4.3. Effect of arid advection on energy partitioning

Because of the influence of arid advection induced by surface heterogeneities, desert-oasis agroecosystems can have a more complex energy budget than arid areas (Kool et al., 2018; Cheng et al., 2014; Zhang et al., 2016; Wang et al., 2019). Arid advection is commonly specified as either regional advection or local advection (Tolk et al., 2006). Regional advection is thought to occur at kilometer-scale heterogeneity and can affect the entire irrigated area (Prueger et al., 2012; Mauder et al., 2020). Local advection originates from the adjacent heterogeneity at the hectometer scale in the upwind section of the crop field. In addition, distinct dry and wet zones within a crop field in ecosystems with partial canopy cover, such as row crops or orchards, can cause within-field advection, which occurs on a much smaller scale (Kool et al., 2018). There was a high probability of arid advection in our study area, which can be attributed to the following: 1) there is a lot of Gobi Desert land around the vineyard (Fig. 1a and b), especially in the southwest part of the vineyard (<200 m), resulting in VPD and temperature gradients between the surrounding area and the vineyard; 2) the main wind direction corresponds to the orientation of the Gobi Desert (Fig. 1b); and 3) the use of gully irrigation causes within-field advection from the dry soil surface to the wet soil surface (Kool et al., 2018). Arid advection can alter the partitioning of the surface energy budget (Lee et al., 2004; Evett et al., 2012). The advection of dry and hot air from a warmer to a cooler surface is known to enhance evapotranspiration by providing additional energy and increasing the atmospheric evaporative demand (Kool et al., 2018), which was also reflected in our results because WS was closely related to the flow of dry air. WS

significantly and positively affected LE through VPD and Ta (Figs. 10 and 11). Fig. 8 shows that the energy balance residual became more negative with an increase in advection intensity. In addition, SEM analysis showed that WS had a significant positive effect on Ta.

In this study, the contribution of arid advection to LE (R_{ad}) varied greatly throughout the growing season (Fig. 7; Table 1), which explains the surprising highs and lows in LE ($LE/(R_n-G)$) and H ($H/(R_n-G)$) during 2017 and 2018, respectively. Arid advection mainly occurred at the fruiting stage (both frequency and intensity), which explains why the LE and R_n were comparable in diurnal variations during the fruiting stage (Fig. 5b). Moreover, R_{ad} exceeded 50% (2017: DOY 181; 2018: DOY 256). These results demonstrated that the effects of arid advection on energy partitioning should not be ignored. This suggests that energy-balance-based models can underestimate evapotranspiration if they do not account for arid advection. The estimate of the effect of arid advection in this study was higher than that in croplands (4–28%; Hanks et al., 1971; Ding et al., 2015) and lower than that in well-irrigated alfalfa fields in arid areas (28–90%; Prueger et al., 1996) but comparable to the effect of arid advection in a similar environment (1–50%; Kool et al., 2018; Li and Yu, 2007). This indicated that environmental conditions significantly influence arid advection. It is worth noting that water supply, planting density, and irrigation frequency can also greatly affect arid advection, even in similar environments (Kool et al., 2018).

Moreover, during the midday period, arid advection occurred quickly after irrigation (Fig. 9), indicating that irrigation is an important driving force of arid advection in arid areas (Lee et al., 2004; Zhang et al., 2016). The frequency and intensity of arid advection will increase owing to the irrigation cultivation of grape plants in the study area (Lee

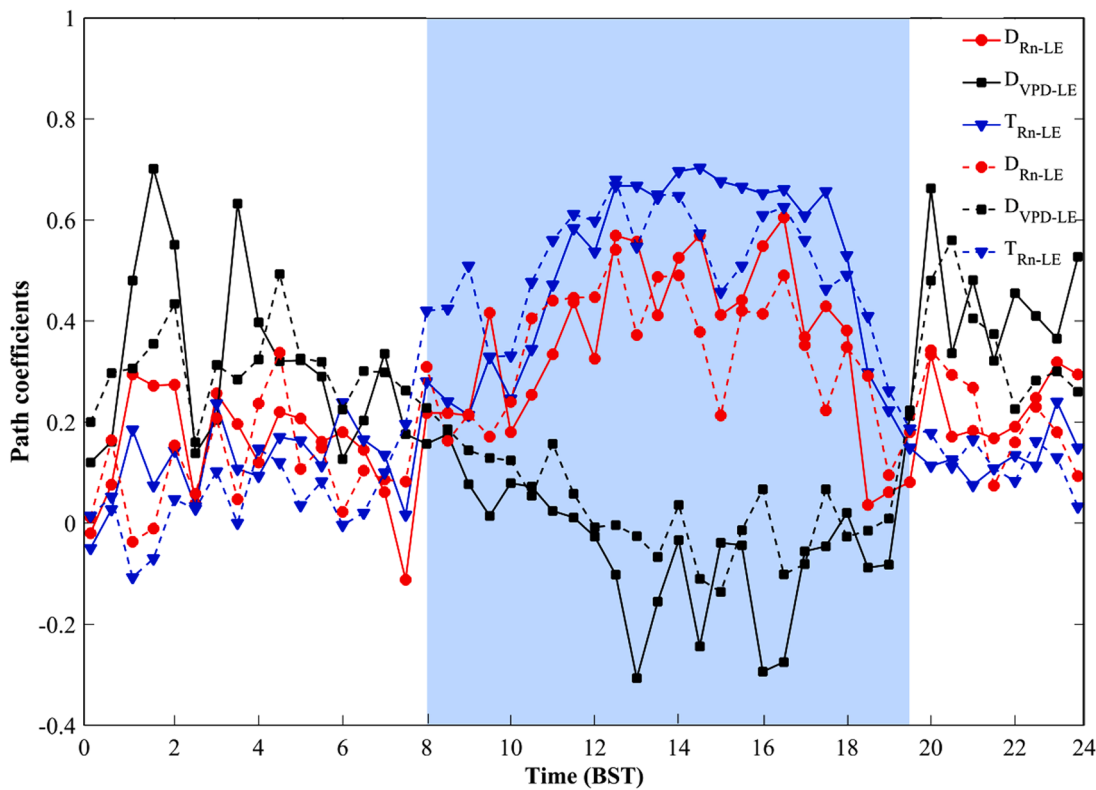


Fig. 12. The average dynamic response of latent heat flux (LE) to net radiation (R_n) and vapor pressure deficit (VPD) in a diurnal cycle in 2017 (solid lines) and 2018 (dotted lines). D_{i-LE} represents the direct effect of i on LE; T_{i-LE} represents the total effect (= direct effect + indirect effect) of i on LE. The blue background indicates the period when the D_{Rn-LE} was greater than the D_{VPD-LE} . Beijing Standard Time (BST) is used here.

et al., 2004). It can be seen from Fig. 9 that the intensity and duration of advection in the subsequent midday period (10:00–16:00) after evening irrigation were lower than those after morning irrigation. A previous study suggested that arid advection can significantly reduce water use efficiency (Li et al., 2007). This means that selecting a reasonable irrigation time should reduce the impact of increased advection on the LE and thus reduce water consumption (Li et al., 2007). Thus, irrigation should be conducted in the evening rather than in the morning in the study region. This may be because the surface heterogeneity at midday was lower with evening than morning irrigation. Without irrigation, the oases would gradually degenerate into deserts (Gao et al., 2002). Regional irrigation alters the energy balance pattern in desert regions and maintains the development of oasis agroecosystems.

4.4. Environmental controls on energy partitioning at different time scales

Environmental factors significantly affect energy partitioning (Zhu et al., 2014; Xie et al., 2018; Li, 2015; Li et al., 2016; Zhang et al., 2016). R_n directly provides available energy ($LE+H$); on the other hand, R_n can increase the leaf temperature, further increasing the transpiration rate to a certain limit (Chen et al., 2014). VPD is another important factor affecting LE, as it is an important indicator of the degree of air dryness and has directly affects stomatal conductance and grape plant transpiration (Liu et al., 2020). Numerous studies have revealed that R_n and VPD are the major environmental factors affecting LE (e.g., Wang et al., 2005; Zhang et al., 2016; Liu et al., 2019; Law et al., 2002; Li et al., 2008; Li, 2015), which is consistent with the results of the SEM analysis in this study (Figs. 10 and 11). The direct effect of VPD on the daily scale was greater than that on the half-hourly scale. This stems from a time lag between VPD and LE at the half-hourly scale (Supplementary Fig. 4), but this time-lag weakened at the daily scale (Supplementary Fig. 5). The degree of influence of R_n on LE decreased with the increasing time scale, and the degree of influence of VPD increased (Li, 2015). Although VPD

directly affected LE, the total effect of R_n was greater than that of VPD, which is consistent with the findings of a previous study (Wang et al., 2005). Moreover, some studies have shown that the main periods controlling LE by R_n and VPD are different within a diel scale (Baldocchi, 1994; Jia et al., 2018; Liu et al., 2021; Li, 2015), but the specific period and influence path remain unclear. In this study, we found that the diurnal variation in LE was mainly affected by VPD through a direct effect from 19:30 to 08:00 and by R_n through direct effects from 08:00 to 19:30 (Fig. 12). R_n determined the energy partitioning into the LE during the daytime and dropped to zero at night, whereas VPD influenced plant transpiration by providing conditions for stomata to open or partially open at night (Baldocchi, 1994). Therefore, it is clear that the main influencing factors have differences in their influence at different timescales. This implies that: 1) The model builder must be aware of this difference when setting up the model, and the user must also be aware when using the model. For example, if a user uses the Priestley–Taylor Jet Propulsion Laboratory (PT-JPL) model to simulate daily evapotranspiration, fundamental errors would occur because the model was designed to simulate monthly evapotranspiration (Fisher et al., 2008). 2) When revealing the potential influence of environmental factors on evapotranspiration or LE, an appropriate timescale should be established, although this is not straightforward.

The role of Ta in affecting LE is more ambiguous than that of R_n and VPD, and it is not always a primary controlling factor (Wang et al., 2014). Several researchers have examined the relationship between soil and leaf temperatures and LE (Mellander et al., 2004; Wieser et al., 2015). Owing to the direct effect of Ta on the VPD change, the significant influence of Ta on LE was mainly due to its indirect effect through VPD, and its direct effect was not significant (Figs. 10 and 11). In addition, Zhou et al. (2019) found that the effect of Ta on the LE decreased with an increase in available water. Our study area was not limited by water, which may be the main reason for the low total effect of Ta compared with that of VPD. P maintained a weak negative effect

on energy exchange during the two years (Figs. 10 and 11), which resulted from fewer rainy events. In general, LE was mainly controlled by radiation energy or available energy rather than water, which was due to the abundant irrigation in the study area (Fig. 2c and d). This result was consistent with α (the average values were 1.24 and 1.33 over the two growing seasons; Supplementary Table 1) because $\alpha > 1$ represents a wet surface with unrestricted water supply and available energy limits LE (Liu et al., 2010; Zhu et al., 2014). In addition, VWC was also considered in our conceptual model (Fig. 4) but not in the final model, which indicated that VWC had no significant impact on LE (Figs. 10 and 11).

The SEM results obtained in this study demonstrate the direct and indirect effects of various environmental factors on LE, indicating a significant advantage of SEM over other methods. The first step in SEM analysis is to establish an appropriate model based on empirical knowledge to use data to verify the causal hypothesis and provide an influence coefficient. This eliminates the shortcomings of traditional statistical methods, that is, the simple use of statistical methods to analyze problems. From the discussion presented above, it is clear that the results of the SEM analysis are consistent with the results of other methods in qualitative terms, which fully demonstrates the rationality of SEM. Most importantly, SEM analysis is an important step forward compared with other methods in that it shows the complex interaction of various factors on the dependent variable. The use of statistical analysis lies between physically based approaches and those related to artificial intelligence, and this study shows that there is room for this intermediate approach.

5. Conclusions

In this study, we investigated variations in energy partitioning and quantified the contribution of arid advection to energy partitioning at different phenological stages in an arid oasis vineyard in northwest China. Furthermore, SEM analysis was used to explore the direct and indirect effects of environmental factors on LE at different timescales. Several conclusions were drawn from this study.

- 1) The energy balance components showed a typical diurnal pattern, with peaks that occurred at around 14:00, except for G , which had a peak delayed by an average of 2 h. LE was the main consumer of available daytime energy during the two growing seasons, even during the shooting and leaf-fall stages. The average $LE/(R_n - G)$ was 0.87 and 0.86 during the two growing seasons. The mean value of β ($= H/LE$) during the entire growing season was only 0.17 in 2017 and 0.16 in 2018.
- 2) The contribution of arid advection to the average daytime LE (with average values of 29% and 25% in the two years) was significant over the entire growing season, especially at the fruiting stage, suggesting that energy balance-based models can underestimate evapotranspiration if they do not account for arid advection. Moreover, arid advection induced by irrigation could be attenuated by selecting a reasonable irrigation time (irrigation at night is more reasonable than irrigation in the morning).
- 3) According to the SEM analysis, R_n had the strongest direct and positive regulation of LE at the half-hourly and daily scales, reflecting energy-limited conditions for LE during the growing season. Furthermore, R_n and VPD mainly directly affected LE; however, there were temporal differences in the order of their influences on LE at the diel scale (0:00–24:00). At the different time scales, the effects of environmental factors on LE showed differences, requiring both the model builder and the user to be aware of these differences.

These findings promote a better understanding of eco-hydrological processes, enabling improved management of water resources in arid areas and providing a reference for simulating surface processes.

CRediT authorship contribution statement

Huiling Chen: Conceptualization, Data curation, Methodology, Project administration, Validation, Writing – review & editing, Writing – original draft. **Yongtai Zhu:** Formal analysis, Project administration, Software, Visualization, Writing – original draft, Writing – review & editing, Investigation. **Gao Feng Zhu:** Funding acquisition, Resources, Supervision, Writing – review & editing. **Yang Zhang:** Resources, Writing – review & editing. **Liyang He:** Investigation. **Cong Xu:** Methodology. **Kun Zhang:** Methodology. **Jing Wang:** Investigation. **Ramamoorthy Ayyamperumal:** Writing – review & editing. **Haochen Fan:** Investigation. **Boyuan Wang:** Investigation.

Declaration of competing interest

The authors declare that they have no known competing financial interests or personal relationships that could have appeared to influence the work reported in this paper.

Data availability

Data will be made available on request.

Acknowledgments

This work was supported by the National Natural Science Foundation of China (No. 42171019), and the Key Project of Natural Science Foundation of Gansu Province of China (23JRRA1025). We thank S. T. Wang for his assistance with field measurements and instrument maintenance.

Supplementary materials

Supplementary material associated with this article can be found, in the online version, at doi:10.1016/j.agrformet.2024.109972.

References

- Alberto, M.C.R., Wassmann, R., Hirano, T., Miyata, A., Hatano, R., Kumar, A., Padre, A., Amante, M., 2011. Comparisons of energy balance and evapotranspiration between flooded and aerobic rice fields in the Philippines. *Agric. Water Manage.* 98 (9), 1417–1430.
- Allen, R.G., Pereira, L.S., Howell, T.A., Jensen, M.E., 2011. Evapotranspiration information reporting: i. Factors governing measurement accuracy. *Agric. Water Manage.* 98 (6), 899–920.
- Baldocchi, D., 1994. A comparative study of mass and energy exchange over a closed C3 (wheat) and an open C4(corn)canopy: I. The partitioning of available energy into latent and sensible heat exchange. *Agric. For. Meteorol.* 67 (3–4), 191–220.
- Baldocchi, D., Falge, E., Gu, L.H., Olson, R., Hollinger, D., Running, S., 2001. FLUXNET: a new tool to study the temporal and spatial variability of ecosystem-scale carbon dioxide, water vapor, and energy flux densities. *Bull. Am. Meteorol.* 82, 2415–2434.
- Baldocchi, D.D., Xu, L.K., Kiang, N., 2004. How plant functional-type, weather, seasonal drought, and soil physical properties alter water and energy fluxes of an oak-grass savanna and an annual grassland. *Agric. For. Meteorol.* 123, 13–39.
- Baldocchi, D.D., Xu, L.K., 2007. What limits evaporation from Mediterranean oakwoodlands—the supply of moisture in the soil, physiological control by plants or the demand by the atmosphere? *Adv. Water Resour.* 30, 2113–2122.
- Chen, D.Y., Wang, Y.K., Liu, S.Y., Wei, X.G., Wang, X., 2014. Response of relative sap flow to meteorological factors under different soil moisture conditions in rainfed jujube (*Ziziphus jujuba* Mill.) plantations in semiarid Northwest China. *Agric. Water Manage.* 136, 23–33.
- Cheng, G.D., Li, X., Zhao, W.Z., Xu, Z.M., Feng, Q., Xiao, S.C., Xiao, H.L., 2014. Integrated study of the water-ecosystem-economy in the Heihe River Basin. *Natl Sci Rev* 1 (03), 413–428.
- Cuxart, J., Wrenger, B., Martínez-Villagrassa, D., Reuder, J., Jonassen, M.O., Jiménez, M.A., Lothon, M., Lohou, F., Hartogensis, O., Dünnermann, J., Conangla, L., Garai, A., 2016. Estimation of the advection effects induced by surface heterogeneities in the surface energy budget. *Atmos. Chem. Phys.* 16, 9489–9504.
- Dare-Idowu, O., Brut, A., Cuxart, J., Tallec, T., Rivalland, V., Zawilski, B., Ceschia, E., Jarlan, L., 2021. Surface energy balance and flux partitioning of annual crops in southwestern France. *Agric. For. Meteorol.* 108529, 308–309.
- De Roo, F., Mauder, M., 2018. The influence of idealized surface heterogeneity on virtual turbulent flux measurements. *Atmos. Chem. Phys.* 18, 5059–5074.

- Díaz-Espejo, A., Fernández, J.E., Verhoef, A., Knight, J.R., Villagarcía, L., 2008. The use of high-resolution weighing lysimeters to improve estimates of soil evaporation in drip-irrigated olive orchards. *Acta Hortic.* 791, 315–320.
- Ding, R.S., Tong, L., Li, F.S., Zhang, Y.Q., Hao, X.M., Kang, S.Z., 2015. Variations of crop coefficient and its influencing factors in an arid advective cropland of northwest China. *Hydrol. Process.* 29 (2), 239–249.
- Ding, R.S., Kang, S.Z., Zhang, Y.Q., Tong, L., Li, S.E., 2014. Characteristics and main controlling factors of water and heat fluxes in maize field in arid inland region. *J. Hydraulic.* 45 (3), 312–319.
- Eichelmann, E., Wagner-Riddle, C., Warland, J., Deen, B., Voroney, P., 2016. Evapotranspiration, water use efficiency, and energy partitioning of a mature switchgrass stand. *Agric. For. Meteorol.* 217, 108–119.
- Evett, S.R., Kustas, W.P., Gowda, P.H., Anderson, M.C., Prueger, J.H., Howell, T.A., 2012. Overview of the bushland evapotranspiration and agricultural remote sensing experiment 2008 (bearex08): a field experiment evaluating methods for quantifying ET at multiple scales. *Adv. Water Resour.* 50 (6), 4–19.
- Fan, Y., Chen, J., Shirkey, G., John, R., Wu, S.R., Park, H., Shao, C., 2016. Applications of structural equation modeling (SEM) in ecological studies: an updated review. *Ecol. Process.* 5 (1), 1–12.
- Ferreira, M.I., Silvestre, J., Conceição, N., Malheiro, A.C., 2012. Crop and stress coefficients in rainfed and deficit irrigation vineyards using sap flow techniques. *Irrig. Sci.* 30 (5), 433–447.
- Foken, T., 2008. The energy balance closure problem: an overview. *Ecol. Appl.* 18 (6), 1351–1367.
- Fisher, J.B., Tu, K.P., Baldocchi, D.D., 2008. Global estimates of the land–atmosphere water flux based on monthly AVHRR and ISLSCP-II data, validated at 16 FLUXNET sites. *Rem. Sens. Environ.* 112, 901–919.
- Gao, X., Mei, X.R., Gu, F.X., Hao, W.P., Gong, D.Z., Li, H.R., 2018. Evapotranspiration partitioning and energy budget in a rained spring maize field on the Loess Plateau. *China. Catena* 166, 249–259.
- Gao, Y.H., Chen, Y.C., Lv, S.H., 2002. Role of irrigation in maintenance and development of modern oasis. *J. Desert Res.* 22 (4), 383–386.
- Grace, J.B., Schoolmaster, D.R., Guntenspergen, G.R., Little, A.M., Mitchell, B.R., Miller, K.M., Schweiger, E.W., 2012. Guidelines for a graph-theoretic implementation of structural equation modeling. *Ecosphere* 3, 1–44.
- Hanks, R.J., Allen, L.H., Gardner, H.R., 1971. Advection and evapotranspiration of wide-row sorghum in the Central Great Plains. *Agron. J.* 63 (4), 520–527.
- Hossen, M.S., Mano, M., Miyata, A., Baten, M.A., Hiyama, T., 2012. Surface energy partitioning and evapotranspiration over a double-cropping paddy field in Bangladesh. *Hydrol. Process.* 26 (9), 1311–1320.
- Helman, D., Osem, Y., Yakir, D., Lensky, I.M., 2017. Relationships between climate, topography, water use and productivity in two key Mediterranean forest types with different water-use strategies. *Agric. For. Meteorol.* 232, 319–330.
- Ingwersen, J., Steffens, K., Högy, P., et al., 2011. Comparison of Noah simulations with eddy covariance and soil water measurements at a winter wheat stand. *Agric. For. Meteorol.* 151, 345–355.
- Jia, G.D., Chen, L.X., Li, H.Z., Liu, Z.Q., Yu, X.X., 2018. The effect of environmental factors on plant water consumption characteristics in a northern rocky mountainous area. *Acta Ecol. Sin.* 38 (10), 3441–3452.
- Jiao, L.J., Ding, R.S., Kang, S.Z., Du, T.S., Tong, L., Li, S.E., 2018. A comparison of energy partitioning and evapotranspiration over closed maize and sparse grapevine canopies in northwest China. *Agric. Water Manag.* 203, 251–260.
- Kool, D., Kustas, W.P., Ben-Gal, A., Lazarovitch, N., Heitman, J.L., Sauer, T.J., Agam, N., 2016. Energy and evapotranspiration partitioning in a desert vineyard. *Agric. For. Meteorol.* 277–287, 218–219.
- Kool, D., Ben-Gal, A., Agam, N., 2018. Within-field advection enhances evaporation and transpiration in a vineyard in an arid environment. *Agric. For. Meteorol.* 255, 104–113.
- Krishnan, P., Meyers, T.P., Scott, R.L., Kennedy, L., Heuer, M., 2012. Energy exchange and evapotranspiration over two temperate semi-arid grasslands in North America. *Agric. For. Meteorol.* 153, 31–44.
- Kutikoff, S., Lin, X., Evett, S., Gowda, P., Moorhead, J., Marek, G., Colaizzi, P., Aiken, R., Brauer, D., 2019. Heat storage and its effect on the surface energy balance closure under advective conditions. *Agric. For. Meteorol.* 265, 56–69.
- Law, B.E., Falge, E., Gu, L., Baldocchi, D.D., Bakwin, P., Berbigier, P., Davis, K., Dolman, A.J., Falk, M., Fuentes, J.D., Granier, A., Hollinger, D., Janssens, I.A., Jarvis, P., Jensen, N.O., Katul, G., Wofsy, S., 2002. Environmental controls over carbon dioxide and water vapor exchange of terrestrial vegetation. *Agric. For. Meteorol.* 113, 97–120.
- Lee, X.H., Yu, Q., Sun, X.M., Liu, J.D., Min, Q.W., Liu, Y.F., Zhang, X.Z., 2004. Micrometeorological fluxes under the influence of regional and local advection: a revisit. *Agric. For. Meteorol.* 122 (1–2), 111–124.
- Lei, H., Yang, D.W., 2010. Interannual and seasonal variability in evapotranspiration and energy partitioning over an irrigated cropland in the North China Plain. *Agric. For. Meteorol.* 150 (4), 581–589.
- Li, L.H., Yu, Q., 2007. Quantifying the effects of advection on canopy energy budgets and water use efficiency in an irrigated wheat field in the North China Plain. *Agric. Water Manage.* 89 (1–2), 116–122.
- Li, S.E., Kang, S.Z., Li, F.S., Zhang, L., 2008. Evapotranspiration and crop coefficient of spring maize with plastic mulch using eddy covariance in northwest China. *Agric. For. Meteorol.* 95 (11), 1214–1222.
- Li, Y., Jing, Y.S., Li, G., Jing, Z.H., 2016. Comparison of energy balance characteristics of cropland on catchment and field scales in low hilly region of red soil. *Chin. J. Ecol.* 35 (09), 2393–2403.
- Li, Y.J., 2015. Environmental controls on water and heat exchanges over rainfed maize cropland in northeast China. *Clim. Environ. Res.* 20 (1), 71–79.
- Liu, S., Li, S.G., Yu, G.R., Asanuma, J., Sugita, M., Zhang, L.M., Hu, Z.M., Wei, Y.F., 2010. Seasonal and interannual variations in water vapor exchange and surface water balance over a grazed steppe in central Mongolia. *Agric. Water Manage.* 97 (6), 857–864.
- Liu, B., Cui, Y.L., Luo, Y.F., Shi, Y.Z., Liu, M., Liu, F.P., 2019. Energy partitioning and evapotranspiration over a rotated paddy field in Southern China. *Agric. For. Meteorol.*, 107626, 276–277.
- Liu, B., Zhao, W.Z., Wen, Z.J., Zhang, Z.H., 2014. Response of water and energy exchange to the environmental variable in a desert-oasis wetland of Northwest China. *Hydrol. Process.* 28, 6098–6112.
- Liu, H., Zhang, Q.L., Tian, Y., 2021. Transpiration characteristics and influencing factors of natural Larix gmelinii stand. *J. Northwest A & F Univ. (Nat. Sci. Ed.)* 49 (10), 56–63.
- Liu, D., Li, Y., Wang, T., Peylin, P., MacBean, N., Ciais, P., Jia, G.S., Ma, M.G., Ma, Y.M., Shen, M.G., Zhang, X.Z., Piao, S.L., 2018. Contrasting responses of grassland water and carbon exchanges to climate change between Tibetan Plateau and Inner Mongolia. *Agric. For. Meteorol.* 249, 163–175.
- Liu, Y., Kumar, M., Katul, G.G., Feng, X., Konings, A.G., 2020. Plant hydraulics accentuates the effect of atmospheric moisture stress on transpiration. *Nat. Clim. Change.* 10 (7), 691–695.
- Ma, J.Y., Zha, T.S., Jia, X., Tian, Y., Bourque, C.P.-A., Liu, P., Bai, Y.J., Wu, Y.J., Ren, C., Yu, H.Q., Zhang, F., Zhou, C.X., Chen, W.J., 2018. Energy and water vapor exchange over a young plantation in northern China. *Agric. For. Meteorol.* 263, 334–345.
- Ma, N., Wang, N., Zhao, L.Q., Zhang, Z.Y., Dong, C.Y., Shen, S.P., 2014. Observation of megadune evaporation after various rain events in the hinterland of Badain Jaran Desert. *China. Sci. Bulletin.* 59, 162–170.
- Mauder, M., Foken, T., Cuxart, J., 2020. Surface-energy-balance closure over land: a review. *Bound. Layer Meteorol.* 177, 395–426.
- McNaughton, K.G., 1976. Evaporation and advection I: evaporation from extensive homogeneous surfaces. *Q. J. R. Meteorol. Soc.* 102 (431), 181–191.
- McNaughton, K.G., Jarvis, P.G., 1983. Chapter 1—predicting effects of vegetation changes on transpiration and evaporation. *Adv. Ecol. Res.* 7 (2), 1–47.
- Mellander, P.E., Bishop, K., Lundmark, T., 2004. The influence of soil temperature on transpiration: a plot scale manipulation in a young Scots pine stand. *For. Ecol. Manage.* 195, 15–28.
- Monteith, J.L., Unsworth, M.H., 2008. *Principles of Environmental Physics*. Academic Press, New York, USA. Third edition.
- Morrison, T., Pardyjak, E.R., Mauder, M., Calaf, M., 2022. The heat-flux imbalance: the role of advection and dispersive fluxes on heat transport over thermally heterogeneous terrain. *Bound. Layer Meteorol.* 183, 227–247.
- Oncley, S.P., Foken, T., Vogt, R., et al., 2007. The Energy Balance Experiment EBEX-2000. Part I: overview and energy balance. *Bound. Layer Meteorol.* 123, 1–28.
- Priestley, C.H.B., Taylor, R.J., 1972. On the assessment of surface heat flux and evaporation using large-scale parameters. *Monthly Weather Rev.* 100, 81–92.
- Prueger, J.H., Hipps, L.E., Cooper, D.I., 1996. Evaporation and the development of the local boundary layer over an irrigated surface in an arid region. *Agric. For. Meteorol.* 78 (3–4), 223–237.
- Prueger, J.H., Alfieri, J.G., Hipps, L.E., Kustas, W.P., Chavez, J.L., Evett, S.R., Anderson, M.C., French, A.N., Neale, C.M.U., McKee, L.G., Hatfield, J.L., Howell, T.A., Agam, N., 2012. Patch scale turbulence over dryland and irrigated surfaces in a semi-arid landscape under advective conditions during BEAREX08. *Adv. Water Resour.* 50, 106–119.
- Qiu, H.Z., Lin, B.F., 2019. *Principle and Application of Structural Equation Model*. China Light Industry Press, Beijing.
- Schmid, H.P., 1994. Source areas for scalars and scalar fluxes. *Bound. Layer Meteorol.* 67 (3), 293–318.
- Suyker, A.E., Verma, S.B., 2008. Interannual water vapor and energy exchange in an irrigated maize-based agroecosystem. *Agric. For. Meteorol.* 148 (3), 417–427.
- Spano, D., Duce, P., Snyder, R.L., 2004. Estimate of mass and energy fluxes over grapevine using eddy covariance technique. *Acta Horticult. (ISHS)* 664, 631–638.
- Tolk, J.A., Evett, S.R., Howell, T.A., 2006. Advection influences on evapotranspiration of alfalfa in a semiarid climate. *Agron. J.* 98 (6), 1646–1654.
- Verma, S.B., Rosenberg, N.J., Blad, B.L., 1978. Turbulent exchange coefficients for sensible heat and water vapor under advective conditions. *J. Appl. Meterol.* 17 (3), 330–338.
- Wang, H.L., Guan, H.D., Deng, Z.J., Simmons, C.T., 2014. Optimization of canopy conductance models from concurrent measurements of sapflow and stem water potential on Drooping Sheoak in South Australia. *Water Resour. Res.* 50, 6154–6167.
- Wang, Q.G., Kellomaki, S., 2005. Role of solar radiation and water vapour pressure deficit in controlling latent heat flux density in a scots pine forest. *Bound. Layer Meteorol.* 115, 131–149.
- Wang, S.T., Zhu, G.F., Xia, D.S., Ma, J.Z., Han, T., Ma, T., Zhang, K., Shang, S.S., 2019. The characteristics of evapotranspiration and crop coefficients of an irrigated vineyard in arid Northwest China. *Agric. Water Manage.* 212, 388–398.
- Wohlfahrt, G., Irschick, C., Thaler, B., et al., 2010. Insights from independent evapotranspiration estimates for closing the energy balance: a grassland case study. *Vadose Zo J.* 9, 1025–1033.
- Wieser, G., Grams, T.E.E., Matyssek, R., Oberhuber, W., Gruber, A., 2015. Soil warming increased whole-tree water use of *Pinus cembra* at the treeline in the Central Tyrolean Alps. *Tree Physiol.* 35, 279–288.
- Wilson, K., Goldstein, A., Falge, E., Aubinet, M., Baldocchi, D., Berbigier, P., Bernhofer, C., Ceulemans, R., Dolman, H., Field, C., Grelle, A., Ibrom, A., Law, B.E., Kowalski, A., Meyers, T., Moncrieff, J., Monson, R., 2002. Energy balance closure at FLUXNET sites. *Agric. For. Meteorol.* 113, 223–243.

- Xu, Z.W., Ma, Y.F., Liu, S.M., Shi, W.J., Wang, J.M., 2017. Assessment of the energy balance closure under advective conditions and its impact using remote sensing data. *J. Appl. Meteorol. Climatol.* 56 (1), 127–140.
- Xie, Y., Wen, J., Liu, R., et al., 2018. Analysis of water vapour flux between alpine wetlands underlying surface and atmosphere in the source region of the Yellow River. *Sci. Cold Arid Reg.* 10 (4) <https://doi.org/10.3724/SP.J.1226.2018.00305>, 0305–0316.
- Yan, C.H., Zhao, W.L., Wang, Y., Yang, Q.X., Zhang, Q.T., Qiu, G.Y., 2017. Effects of forest evapotranspiration on soil water budget and energy flux partitioning in a subalpine valley of China. *Agric. For. Meteorol.* 246, 207–217.
- Yang, F.L., Zhou, G.S., 2011. Characteristics and modeling of evapotranspiration over a temperate desert steppe in Inner Mongolia, China. *J. Hydrol.* 396, 139–147.
- Yu, Z.J., Hu, X.T., R, H., Wang, X.M., Wang, W.E., He, X.X., 2020. Characteristics of water heat flux in vineyard in semi-humid area and its responses to environmental factors. *Water Saving Irrig.* 4 (02), 96–101.
- Zhang, B.Z., Kang, S.Z., Zhang, L., Du, T.S., Li, S.E., Yang, X.Y., 2007. Estimation of seasonal crop water consumption in a vineyard using Bowen ratio-energy balance method. *Hydrol. Process.* 21 (26), 3635–3641.
- Zhang, Y.Y., Zhao, W.Z., 2015. Vegetation and soil property response of short-time fencing in temperate desert of the Hexi Corridor northwestern China. *Catena* 133, 43–51.
- Zhang, Y.Y., Zhao, W.Z., He, J.H., Zhang, Kun., 2016. Energy exchange and evapotranspiration over irrigated seed maize agroecosystems in a desert-oasis region, northwest China. *Agric. For. Meteorol.* 223, 48–59.
- Zhao, X.S., Liu, Y.B., 2018. Variability of surface heat fluxes and its driving forces at different time scales over a large ephemeral lake in China. *J. Geophys. Res.* 123, 4939–4957.
- Zhao, P., Zhang, X.T., Li, S.E., Kang, S.Z., 2017. Vineyard energy partitioning between canopy and soil surface: dynamics and biophysical controls. *J. Hydrometeorol.* 18 (7), 1809–1829.
- Zhou, S.Q., Wang, J., Liu, J.X., Yang, J.H., Xu, Y., Li, J.H., 2012. Evapotranspiration of a drip-irrigated, film-mulched cotton field in northern Xinjiang, China. *Hydrol. Process.* 26 (8), 1169–1178.
- Zhou, L., Wang, Y., Jia, Q.Y., Li, R.P., Zhou, M.Z., Zhou, G.S., 2019. Evapotranspiration over a rainfed maize field in northeast China: how are relationships between the environment and terrestrial evapotranspiration mediated by leaf area? *Agric. Water Manage.* 221, 538–546.
- Zhu, G.F., Lu, L., Su, Y.H., Wang, X.F., Cui, X., Ma, J.Z., He, J.H., Zhang, K., Li, C.B., 2014. Energy flux partitioning and evapotranspiration in a sub-alpine spruce forest ecosystem. *Hydrol. Process.* 28 (19), 5093–5104.